Journal of Engineering and Applied Sciences 13 (24): 10221-10231, 2018
ISSN: 1816-949X

Corrosion Protection of 316L Stainless Steel by HA Coating via. Pulsed Laser Deposition Technique

Abdul Wahid Rajih, Nawal Mohammed Dawood and Farah Sami Rasheed
College of Materials Engineering, University of Babylon, Hillah, Babil, Iraq

Abstract: Austenetic stainless steel AISI 316L are frequently used as orthopedic implants because their mechanical properties and formability. In this research, a film of Hydroxyapatite (HA) was prepared by a PLD technique on 316L SS. HA was pressed at pressure (150 MPa) with partical size (2.745 μm) and used as a target in the coating. Effects of the number pulses (3000, 4500 and 6000) on the coating layer properties have been studied. Effects of the annealing temperature (450°C) for 1 h and under an empty atmosphere on the coating layer properties have been studied, also. The microstructure and composition of the coating were analyses by Scanning Electron Microscopy (SEM), Energy Dispersive Spectroscopy (EDS) and X-Ray Diffraction (XRD). The mechanical property of the coating was evaluated by Vickers micro hardness test. The electrochemical corrosion behaviors and Ni ions release of uncoated and coated samples with different number of pulses in synthetic saliva and hanks solution were also, investigated. The XRD analysis of coated sample indicate the formation of the HA layer. SEM results shows evident improvement in microstructure and grow HA film with increasing in pulses number. In bioactivity test the percentage of (Ca) and (P) are increased significantly after 14 days immersion in SBF which confirms that the samples are bioactive. A significant corrosion test results show that the corrosion rate after HA coating decreased from (2.1370*10-3 mpy) for uncoated sample into (0.05110*10-3 mpy) for coated sample in synthetic saliva. And from (9.26221*10-3 mpy) for uncoated sample into (0.34206*10-3 mpy) for coated sample in Hanks solution. The Ni release test shows that the amount of releasing Ni decreased from (0.56716 ppm) for uncoated samples into (0.11940 ppm) for coated sample in synthetic saliva. And Ni ions decreased from (10.4179 ppm) for uncoated samples into (0.2686 ppm) for coated sample in Hanks solution and another interesting increase in biocompatibility was achieved during the research for the coated sample compare to the uncoated 316L stainless steel sample.

Key words: St.St.316L, pulsed laser, annealing, hydroxyapatite, Stimulated Body Fluid (SBF), bioactivity

INTRODUCTION

The 316L Stainless Steel (SS) is used for restoration of anatomical structure because of its high mechanical strength, good biocompatibility and cost effective. It is widely used in the orthopedic surgeries such as joint replacement and fracture fixation (Hermawan *et al*., 2011). The corrosion rate of metallic implant in the human body must be negligible. Over the past two decades, the ion release and corrosion properties of metallic implant materials under physiological conditions have been extensively studied under physiological conditions (Okazaki *et al*., 2004). The release of iron, nickel and chromium from the implant leads to unwanted reaction around the implanted area which may cause permanent implant failure. Thus, the corrosion-resistant coating and surface modification of the implant are required .Coating of bioactive materials using Hydroxyapatite (HA) in the metallic implant has many advantages including improved corrosion resistance of implant surface and enhanced bio interaction with the surrounding tissues (Smausz *et al*., 2004). HA is one of the naturally available biocompatible and bioactive materials that show the ability to interact with surrounding bone. A coatings on metallic substrates have been produced by a wide range of deposition techniques including pulsed laser deposition, electrophoretic and electron beam deposition, plasma spraying and ion implantation (Puleo and Huh, 1995). Pulsed Laser Deposition (PLD) has attracted interest due to its versatility and controllability as well as its ability to synthesize and deposit uniform films with an accurate control of the stoichiometry and crystallinity (Balla *et al*., 2013; Kwok *et al*., 2009; Ng *et al*., 2011). This study investigates the use of an Nd:YAG laser operating in pulsed mode for fabricating bioactive HA coatings on 316L stainless steel. The corrosion behavior, ions release and apatite-forming ability of the HA coated 316L stainless steel specimens will be studied.

Corresponding Author: Farah Sami Rasheed, Department of Ceramics and Building Materials, University of Babylon, Hillah, Babil, Iraq

Table 1: Chemical analysis of St.St 316L

Element	C	Si	Mn	P	S	Cr	Mo	Ni	Al	Co	Cu	V	Fe
Percentage	0.023	0.322	1.00	0.038	0.00	17.91	2.06	9.85	0.001	0.153	0.286	0.112	Bal

MATERIALS AND METHODS

Powder and target preparation: A 20 g of HA powder was collected and processed beginning with manual grinding using mortar to get the semi-finished powder. The powder was sieved using sieve number of (200) meshes. The resulted powder was crushed and milled to obtain a nano-size powder by using of a planetary ball milling,. The milling was done for 24 h at 350 rpm. The particle size of the powder obtained from milling process was measured using particle size analyzer Bettersize 2000 laser particle size analyzer. The powder was (0.668-12.99) μm. Then, the powder was mixed with (3 mL) of Poly Vinyl Alcohol (PVA) as a binding material. Then, the mixture was mold in (Ø 20 mm) and pressed at pressures (150 MPa), after that, the target was dried using the dry box at 150°C for 4 h for dehumidify and PVA releasing.

Preparation of St.St.316L substrates: The 316 L St.St. plate with diameter of 12 mm was cut into 3 mm thickness samples. The chemical composition of the 316L St.St plate was done in state company for Inspection and Engineering Rehabilitation (SIER)/Ministry of Industry and Minerals. Table 1 shows the chemical analysis of 316L St.St. The samples were wet ground using 120, 220, 320, 600, 1000, 1200 and 2000, grit silicon carbide papers, the samples were then cleaned for 10 min in each of distilled water, acetone and ethanol, respectively using ultra sound cleaning device.

Pulsed laser deposition PLD process: In this step, targets were placed onto a rotating holder Fig. 1 and ablated using excimer lasers with pulses of ArF (λ = 1064 nm) and applied energy of (600) mJ. The ablated area was approximately 20 mm^2 and the number of pulses was in the (1500-6000) range. Thin layers were deposited onto St.St.316l substrate heated at t temperature 300°C. Target substrate distance was set to 3 cm and the pressure in the PLD chamber was 1.5×10-5 torr. The samples coding shown in Table 2.

Annealing process: The deposited films were post-annealed at temperature 450°C for 1 h in vacuum furnace at heating rate 5°C/min.

Categorization

X-Ray Difraction (XRD): X-ray diffraction of powders and composite material were identified with XRD-system type (DX-2700, X-ray diffractometer, using Cu Kα radiation (λ = 1.5405 Å) and a scanning speed of 5θ°/min from (10-90°) of 2θ (Bragg angle).

Table 2: Samples coding

Sample code	A	B1	B2	B3
Number of pulses	Uncoated	3000	4500	6000

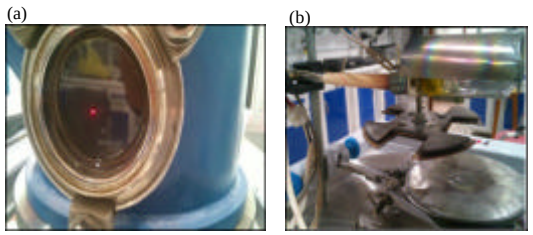

Fig. 1a: Deposition chamber and b) Base of the deposition chamber

SEM analysis: The microstructure and topography of the films were examined using Scanning Electron Microscopy (SEM) and combination EDS analysis

AFM analysis: The depth morphology, roughness of surface thin film was investigated with a type AA3000 Angstrom advanced Inc Atomic Force Microscope (AFM).

Thickness analysis: The film thickness measured by thickness measuring device. Calibrated digital coating thickness gauge model (TT260-A071809290) time group Inc.

Energy Dispersive Spectroscopic (EDX): Energy Dispersive X-Ray (EDX-7000) was used to analyze the chemical composition of sample surface before and after immersion in SBF for duration 3, 7 and 14 days, respectively.

Bioactivity estimation (*in vitro*): The prepared samples were immersed for (3, 7, 14) days in Simulated Body Fluid (SBF) that has inorganic ions concentration similar to those of human extracellular fluid. The ions concentration of SBF is given in Table 3 nearly equal to those of human blood plasma.

Preparation of Stimulated Body Fluid (SBF): SBF is a metastable solution containing calcium and phosphate ions already supersaturated with respect to the apatite.

Table 3: Alchemical combination of stimulated body fluid solution .

Demand	1	2	3	4	5	6	7	8
Substance	NaCl	$NaHCO_3$	KCl	$Na_2HPO_4.2H_2O$	$MgCl_2.6H_2O$	$CaCl_2.2H_2O$	Na_2SO_4	$(CH_2OH)_3CNH_2$
Quantity	6.547	2.268	0.373	0.178	0.305	0.368	0.071	6.057

Table 4: Results of EDX analysis for B3 sample

Measurement Condition

Instrumen t: EDX-7000 Atmosphere: Air Collimator: 10(mm)

Analyte	TG kV uA	FI Acq.(keV)	Anal.(keV)	Time(sec)	DT (%)
Na-Sc	Rh 15 65-Auto	0 - 2 0	0.00- 4.40	Live- 100	30
Al-U	Rh 50 9-Auto	0 - 4 0	0.00-40.00	Live- 100	29

Quantitative Result

Analyte	Result	[3-sigma]	Proc.-Calc . Line	Int.(cps/uA)
Fe	67.721%	[0.111]	Quan-FP FeKa	3751.5560
Cr	17.085o.	[0.049]	Quan-FP CrKa	1206.7852
Ni	9.415%	[0.051]	Quan-FP NiKa	344.2946
Si	1.351%	[0.189]	Quan-FP SiKa	0.1547
Mo	1.241%	[0.008]	Quan-FP MoKa	203.2511
Mn	1.120%	[0.007]	Quan-FP MnKa	77.9553
P	0.850%	[0.089]	Quan-FP P Ka	0.3019
Ca	0.621%	[0.009]	Quan-FP CaKa	3.9280
Cu	0.396%	[0.007]	Quan-FP CuKa	16.9738
K	0.097%	[0.013]	Quan-FP K Ka	0.3715
V	0.051%	[0.006]	Quan-FP V Ka	2.8483
Bi	0.051•6	[0.006]	Quan-FP BiLa	2.0539

Therefore, SBF is prepared as follows: reagents (Table 3) were sequentially added to 700 mL of H_2O with the restriction that a new precursor (Table 4) was added only after the previous addition had completely dissolved.

A total of 40 mL of 1M HCl solution was used for pH adjustments during the preparation of 1 L of SBF solution. 15 mL of this acid solution was added just before the addition of 6th reagent ($CaCl_2.2H_2O$) in order to avoid turbity. After addition of the 8th reagent ($(CH_2OH)_3CNH_2$), the solution temperature was raised from ambient to 37°C. It was then titrated with 1M HCl to a pH of 7.4 at 37°C. During titration process, it was required to dilute the solution with consecutive additions of de-ionized water in order to make the final volume to 1 L.

The prepared sample of SBF solutions is to be capable of being stored at 5°C for a month without degradation. The simulated body fluid, solution was changed every 4 days to provide constant chemical composition of solution (Ohtsuki, 2011).

Hardness test: Vickers hardness (TH-717 digital micro vickers hardness tester) was used to measure the hardness of HA thin film, at load (1.96 N) and holding time 15 sec.

Electrochemical test

Solutions: Solutions used in this research were artificial saliva and Hank's solution (chemical composition is shown in Table 3 and 4 with the pH of artificial saliva and Hank's solution at 37°C were 6.7 and 7.4, respectively.

Open Circuit Potential (OCP): The aim of the OCP-time measurement is to understand the corrosion behavior of the coated and uncoated specimens under equilibrated conditions in artificial saliva and Hank's solution. The OCP-time measurement is considered as an important parameter for evaluating the stability of the passive film of the specimens. The tests were carried out with the samples immersed in a Hank's solution and artificial saliva. The potential of the working electrode is measured with respect to a Saturated Calomel Electrode (SCE). A voltmeter is connected saturated between the working electrode and the reference electrode. For each specimen 3 h open circuit potential measurement was performed. The first record was taken immediately after immersion then the voltage was monitored for the intired period of test at an.

Potentiostatic polarization: Electrochemical experiments were performed in three electrode cell containing and electrolytes similar to nature saliva and Hank's solution. The counter electrode was Pt electrode and the reference electrode was SCE and working electrode (specimen) according to the American Society for Testing and Materials (ASTM). The potentiodynamic polarization curves were plotted and both corrosion current density (Icorr) and corrosion potential were estimated by Tafel plots by using anodic and cathodic branches. The test was conducted by stepping the potential using a scanning rate 0.4 mV/sec from initial potential of 250 mV below the open circuit potential and the scan continued

up to 250 mV above the open circuit potential. Corrosion rate measurement is obtained by applying the following equation (Shalabi *et al*., 2007):

$$\text{Corrosion rate (mpy)} = 0.13\text{icorr(E.W.)}/A\rho \quad (1)$$

Where:

EW = Equivalent Weight (g/eq)
A = Area (cm^2)
ρ = Density (g/cm^3)
0.13 = Metric and time conversion factor
icorr. = Current density ($\mu A/cm^2$)

The improvement percentage is calculated for samples with coating, using the following equation (Ng, 2011):

$$\text{Improvement percentage} = CR_0\_CR/CR_0 \times 100 \quad (2)$$

Where:

CR_0 = The corrosion rate of master sample (without coated)
CR = The corrosion rate of coated sample (with HA coated)

The release of Ni ions: This test was achieved by using atomic absorption spectroscopy device. In order to determine the amount of Ni ions leached from the coated and uncoated 316l st.st samples into saliva and Hank's solution. The dissolution test was used to measure the ions in both solutions from the samples immersed for 2 weeks at 37°C. A sample of each type, uncoated and coated HA coating (3000, 4500 and 6000) PLD samples are immersed in 50 mL of saliva and Hanks solution in Poly Propylene (PP) bottles. The (PP) bottles are closed tightly and incubated in the thermostatic chambers at 37°C for 2 weeks. All bottles were shaken gently for a few seconds every 3 days. After 2 weeks, the saliva and Hank's solution in the bottles are analyzed by atomic absorption spectroscopy to determine the amount of Ni ions leached from each specimen.

RESULTS AND DISCUSSION

X-ray diffraction: Figure 2 and 3 show the hydroxyapatite and the XRD results of the HA thin films after annealing in the range of 10-50° diffracted angle. The pattern refers to the existence peaks of HA phase Ca10

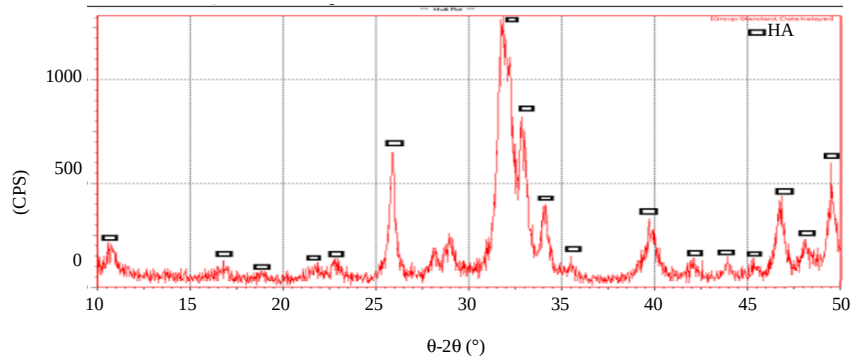

Fig. 2: XRD pattern of HA powder

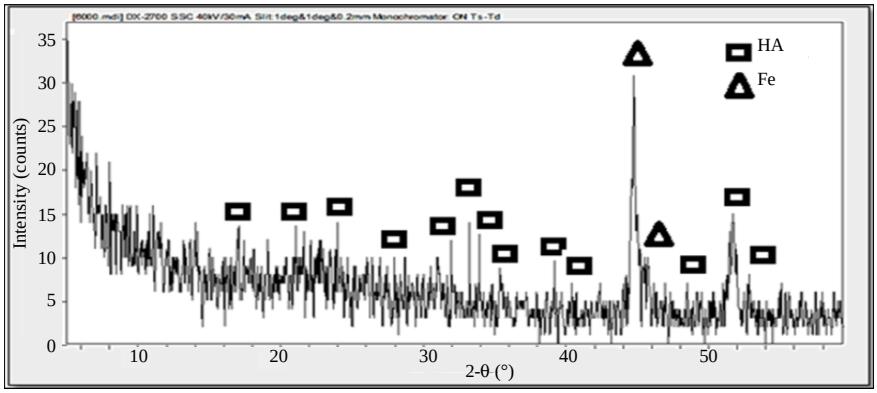

Fig. 3: XRD analysis of HA film

$(PO_4)6(OH)_2$. The observed positions of the diffraction lines (2θ and corresponding d for the patterns shown in Fig 2 and 3 are in full agreement with the corresponding values reported for hexagonal hydroxyapatite (JCPDS, C and No. 09-0432) shown in Fig. 4.

SEM results: Figure 5 shows SEM micrographs of 150 MPa HA samples deposited at different pulses and at 300°C substrate temprature and 550°C annealing temp. It is clear the effect of pulses increasing the improvement of the microstrucrture of the HA films. The HA particles deposited are grown to form clusters and seems to form a dense aggregated structure on the substrate, furthermore, more pulses will be beneficial in improving the film growing, density and microstructure.

AFM results: Figure 6 and 7 show results from AFM of HA coating deposited at different pulses laser before and after annealing annealing. It can be noticed that deposition rate of HA particles is affected by increasing the pulses laser to (6000). It can be seen that the roughness decreased with the pulses increasing to (6000) and the roughness decreased before annealing to (5.26 nm) and then increased to (30.3 nm) with increasing temperatures after annealing and this result in agreement with Samausz *et al*. (2004), Fig. 6 and 7 show the effect of number of pulses on surface roughness of HA coating before and after annealing (Fig. 8 and 9).

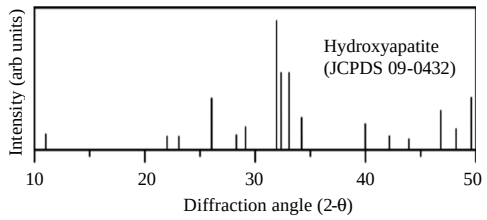

Fig. 4: XRD standard card for HA

Thickness results: The effect of laser pulses number on HA film thickness is shown in Fig. 10. For B1 sample the thickness is 47.8 μm. The thickness increased to 48.5 μm for B2 sample and then the thickness reach to it is high value 49.7 μm for B3 sample. Anyhow, with increasing number of laser pulses, the deposition rate increased and the thickness increased also.

EDX results: The percentages of (Ca) and (P) in HA films are increased with increase immersion time (3, 7 and 14 days), respectively as shown in Fig. 11 according to the results in Table 4-7 for the B3 sample. It will be interesting to know that the increasing of percentages is very slightly after 3 days in comparison with those after 7-14 days. This is due to intervals reduction resulted in reduce drown ions from SBF solution. This is agreement with the finding of reference (Ghaith *et al*., 2015).

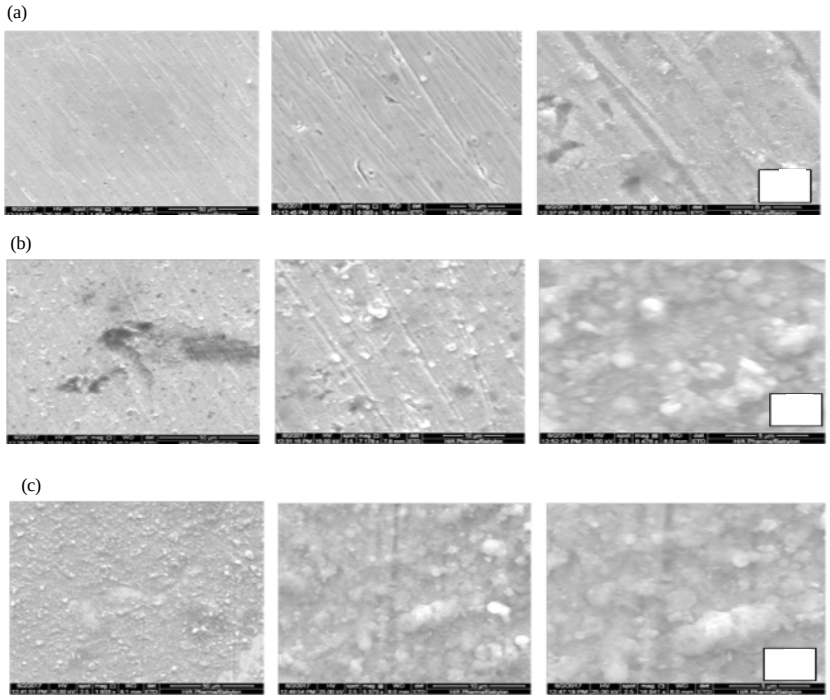

Fig. 5: SEM Micrographs of samples: a) B1; b) B2 and (c) B3

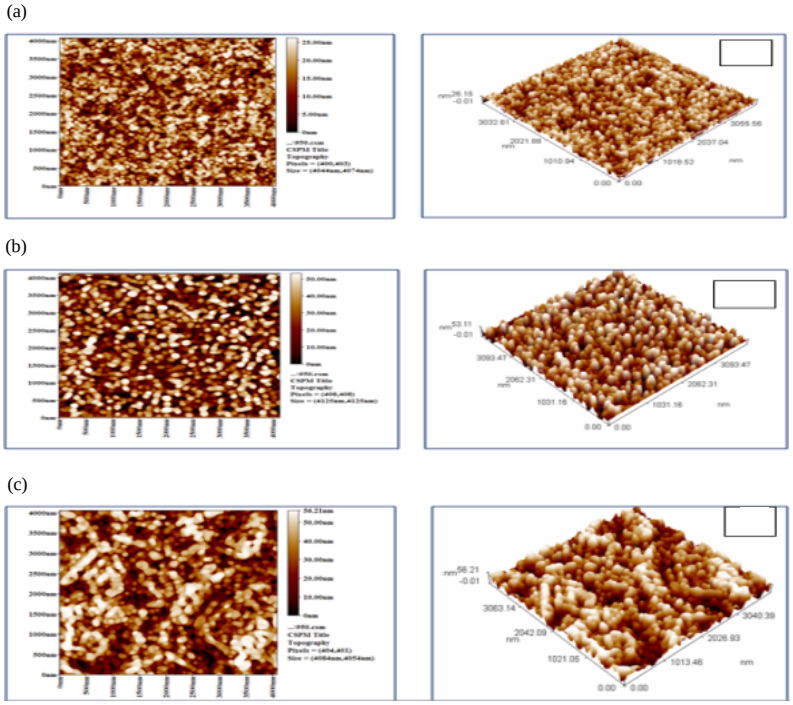

Fig. 6: AFM pattern of 150 MPa samples at: a) B1; b) B2 and c) B3 before the annealing

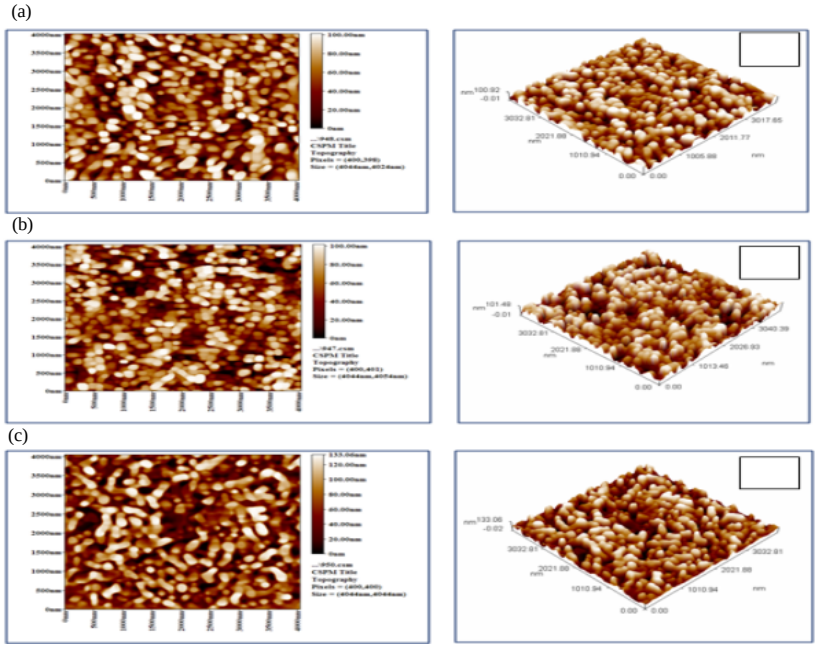

Fig. 7: AFM pattern of 150 MPa samples at: a) B1; b) B2 and c) B3 after the annealing

Hardness resuls: The effect of laser pulses number on the HA coating hardness are shown in Fig. 12, the significant effect of pulses number on the resulted hardness. can be observed. Hardness of uncoated samples are improved after coating it with HA, furthermore increasing of pulses from 3000-6000 could improve the hardness from (310-420 HV), this results are agreement with Rajesh *et al.* such improvement observed in SEM results as in Fig. 11. Most likely the pulse increasing could implant more HA particles on the substrate surfaces again.

Table 5: Results of EDX analysis for B3 sample an immersed for 3 days in SBF solution

Measurement Condition

Instrument: EDX-7000 Atmosphere: Air Collimator:10 (mm)

Analyte	TG kV	uA FI	Acq.(keV)	Anal.(keV)	Time (sec)	DT (%)
Al-U	Rh 50	8-Auto	--- 0 - 4 0	0.00-40.00	Live- 100	31
Na-Sc	Rh 15	56-Auto	--- 0 - 2 0	0.00- 4.40	Live- 100	30

Quantitative Result

Analyte	Result	[3-sigma]	Proc.-Calc .	Line	Int.(cps/uA)
Fe	65.744%	[0.104]	Quan-FP	FeKa	4477.9744
Cr	16.916%	[0.047]	Quan-FP	CrKa	1429.7657
Ni	9.359%	[0.048]	Quan-FP	NiKa	428.9210
P	2.922%	[0.085]	Quan-FP	P Ka	1.2986
Ca	1.405%	[0.015]	Quan-FP	CaKa	10.7604
Mo	1.232%	[0.008]	Quan-FP	MoKa	252.9362
Mn	1.046%	[0.006]	Quan-FP	MnKa	88.2150
Si	0.895%	[0.169]	Quan-FP	SiKa	0.1281
Cu	0.382%	[0.006]	Quan-FP	CuKa	20.5083
V	0.056%	[0.006]	Quan-FP	V Ka	3.7250
Bi	0.043%	[0.006]	Quan-FP	BiLa	2.2046

Table 6: Results of EDX analysis for B3 sample an immersed for 7 days in SBF solution

Measurement Condition

Instrument: EDX-7000 Atmosphere: Air Collimator:10 (mm)

Analyte	TG kV	uA FI	Acq.(keV)	Anal.(keV)	Time (sec)	DT (%)
Al-U	Rh 50	8-Auto	--- 0 - 4 0	0.00-40.00	Live- 100	30
Na-Sc	Rh 15	58-Auto	--- 0 - 2 0	0.00- 4.40	Live- 100	31

Quantitative Result

Analyte	Result	[3-sigma]	Proc.-Calc.	Line	Int.(cps/uA)
Fe	64.858%	[0.105]	Quan-FP	FeKa	4307.2926
Cr	17.011%	[0.049]	Quan-FP	CrKa	1387.5899
Ni	8.886%	[C.047]	Quan-FP	NiKa	401.8321
P	3.579%	[0.096]	Quan-FP	P Ka	1.5700
Ca	1.861%	[0.017]	Quan-FP	CaKa	13.8824
Mo	1.179%	[0.008]	Quan-FP	MoKa	240.2835
Mn	1.097%	[0.007]	Quan-FP	MnKa	89.8328
Si	1.030%	[0.169]	Quan-FP	SiKa	0.1459
Cu	0.346%	[0.006]	Quan-FP	CuKa	18.3426
K	0.088%	[0.011]	Quan-FP	K Ka	0.4000
V	0.063%	[0.006]	Quan-FP	V Ka	4.0326

Table 7: Results of EDX analysis for B3 sample an immersed for 21 days in SBF solution

Measurement Condition

Instrument: EDX-7000 Atmosphere: Air Collimator:10 (mm)

Analyte	TG kV	uA FI	Acq.(keV)	Anal.(keV)	Time(sec)	DT (%)
Al-U	Rh 50	8-Auto	--- 0 - 4 0	0.00-40.00	Live- 100	29
Na-Sc	Rh 15	59-Auto	--- 0 - 2 0	0.00- 4.40	Live- 100	30

Quantitative Result

Analyte	Result	[3-sigma]	Proc.-Calc.	Line	Int.(cps/uA)
Fe	63.480%	[0.105]	Quan-FP	FeKa	4150.2036
Cr	16.728%	[0.049]	Quan-FP	CrKa	1315.1623
Ni	8.914%	[0.048]	Quan-FP	NiKa	401.5076
P	4.547%	[0.111]	Quan-FP	P Ka	1.9728
Ca	2.423%	[0.021]	Quan-FP	CaKa	17.5359
Mo	1.162%	[0.008]	Quan-FP	MoKa	235.5097
Si	1.131%	[0.180]	Quan-FP	SiKa	0.1590
Mn	1.035%	[0.007]	Quan-FP	MnKa	82.4261
Cu	0.381%	[0.006]	Quan-FP	CuKa	20.1177
K	0.143%	[0.014]	Quan-FP	K Ka	0.6298
V	0.056%	[0.006]	Quan-FP	V Ka	3.4339

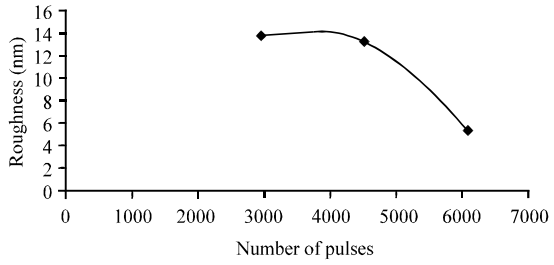

Fig. 8 : The Effect of number of pulses on HA coating surface roughness before annealing

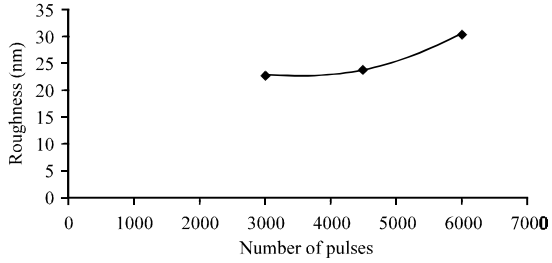

Fig. 9: The effect of number of pulses on HA coating surface roughness after annealing

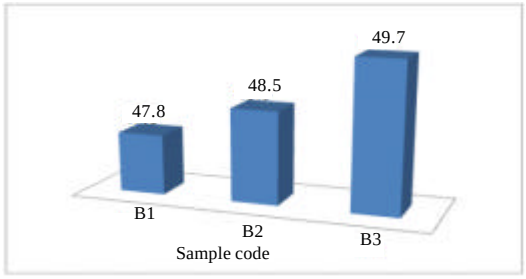

Fig. 10: The thickness of layer HAP coating with various pulses

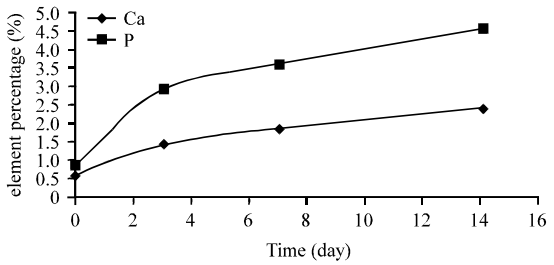

Fig. 11: The percentages of calcium and phosphate of HA films with time after immersion in SBF after 3, 7 and 14 days

Corrosion tests

Open circuit potential (OCP) time measurements: The OCP time was measured with respect to to SCE in

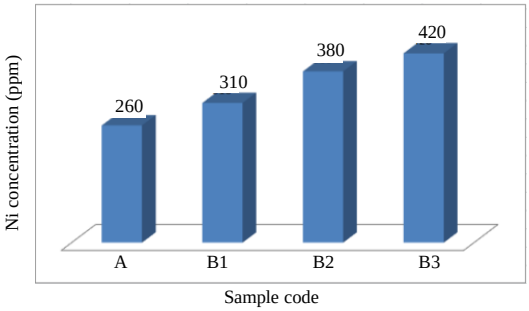

Fig. 12: The effect of laser pulses on HA coating hardness

synthetic saliva and Hank's solution at 37°C for uncoated samples and coated samples (HA coating). The data of OCP are shown in Table 8 and 9.

Potentiostatic polarization: This test was done by using the potentiostatic polarization test in two different solutions (synthetic saliva and Hank's solution) for uncoated and HA coated samples at 37°C. Corrosion parameters (corrosion potential, corrosion current and corrosion rate), extracted from these curves are shown in Table 8. It could be observed that there is a significant shift toward lower current densities of the polarization curves for samples with different pulsed laser number. Icorr. For sample, (B1) are around 0.1051 μA/cm^2 while Icorr. For the sample (B2) are around 0.0348 μA/cm^2 but at (B3) which are much lower than Icorr around 0.016 μA/cm^2. For (A) sample Icorr which are around 0.6691 μA/cm^2. These results indicate stability behavior of HA coating layer. Along with an improvement of corrosion resistance, this HA coating is able to change the properties of the surface on the materials without affecting the properties of the bulk (Shalabi *et al*., 2007; Ajay and Abhinandan, 2010). The corrosion current and calculated corrosion rate are relatively measures of corrosion and illustrate how much material is lost during the corrosion process. Hence, the higher current density and calculated corrosion rate cause more materials lost. HA coating can reduce corrosion rate of the coating implant in human body, hence, reduce the metallic ions release. Properties of HA gave a useful application in coating of porous metallic implants. After implantation of prostheses, a close surface contact between the metallic prosthesis and the surrounding bone tissue is needed for subsequent bone ingrowths. The presence of HA in the coating of the metallic implant leads to a rapid bonding between HA and surrounding bone tissue. Its application in coating implants combines the strength and toughness of the substrate with bioactive characteristics of HA which can induce the surrounding bone tissue in growths

Table 8: Illustrate the corrosion potential (Ecorr.), corrosion current (Icorr.), Corrosion Rate (CR) and improvement percentage of coated samples in synthetic saliva at 37°C

Samples	Sample code	OCP (mV)	Icorr. (μA/cm^2)	Ecorr. (mV)	Corrosion rate (mpy)×10^{-3}	Improvement percentage (%)
A	A	-335	0.6691	-7.80	2.13700	
B	B1	-372	0.1051	-219.70	0.33567	84.29
C	B2	-235	0.0348	-120.00	0.11114	94.76
D	B3	-276	0.0160	-24.50	0.05110	97.60

Table 9: Illustrate the corrosion potential (Ecorr.), corrosion current (icorr.), Corrosion Rate (CR) and improvement percentage of coated samples in Hank's solution at 37°C

Samples	Sample code	OCP (mV)	Icorr. (μA/cm^2)	Ecorr. (mV)	Corrosion rate (mpy)×10^{-3}	Improvement percentage (%)
A	A	-250	2.9000	-113.8	9.26221	
B	B1	-215	0.1500	-0.3	0.47908	94.82
C	B2	-268	0.1225	4.4	0.39125	95.77
D	B3	-210	0.1071	-27.7	0.34206	96.30

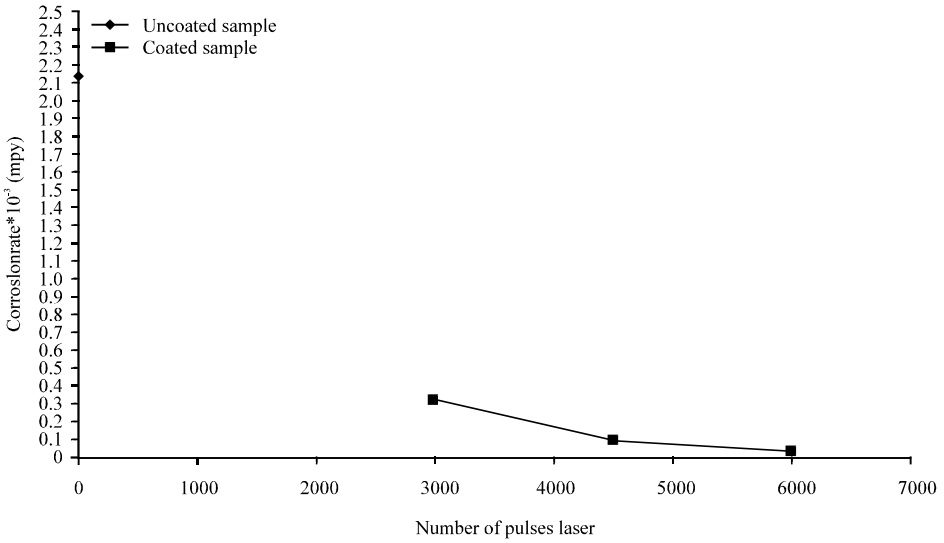

Fig.13: Corrosion rate (mpy) in synthetic saliva at 37°C for the uncoated sample and HA coated samples with various number of puls 3D laser

and future formation of chemical bonding. Also, the presence of HA in coatings can improve corrosion resistance of the coated implant in biological solutions which can reduce metallic release and also, promotes fixation via chemical bonding (Shalabi *et al*., 2007; Smausz *et al*., 2004). The data listed in Table 9 shows the corrosion parameters of HA coated samples in Hank's solution at 37°C. The corrosion potential of all coated samples shows a significant shift to a positive direction and have more noble potential compared to uncoated sample in Table 9. From Table 8, it is clear that (B1-B3) samples have current densities and corrosion rate much lower than current densities and corrosion rate of (A) sample. This belong to the role of HA coating in reducing corrosion resistance for 316 L st.st samples immersion in synthetic saliva at 37°C . The same behavior can be seen in Table 9 for samples immersed in Hank's solution at 37°C. Figure 13 and 14 shows the relationship between corrosion rate and pulsed laser number in synthetic saliva and Hank's solution at 37°C, respectively for HA coated samples. The coated implant material with HA coating , however, attracted more attention to achieve the combination of bioactivity, biocompatibility properties (Singh and Dahotre, 2007). It can be concluded that the HA coating for surface of metallic implant proved to be more corrosion resistance and more favorable surface for getting bone marrow cell attachment than an uncoated 316L stainless steel because HA is known to be an osteon-inductive materials. HA coating attributed to reduce the surfaces area in contact with synthetic saliva and Hank's solution which leads to a decrease in the measured corrosion rate and results are in agreement with other researcher. The improvement percentage of HA coating samples in saliva and Hank's solution are increased with increasing number of pulses laser in the samples. The best improvement percentage for sample in synthetic saliva is (97.60%) at (B3) sample and (96.30%) also for number of pulses laser in Hank's solution. From the Table 9 it can be seen that there is a slightly increasing in corrosion current and corrosion rate for all

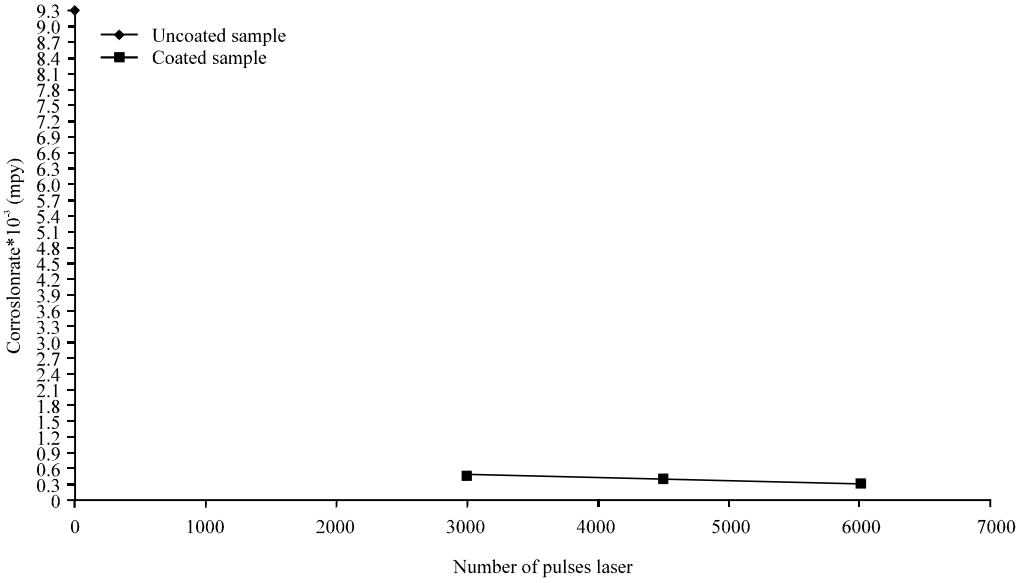

Fig. 14: Corrosion rate (mpy) in Hank's solution at 37°C for the uncoated sample and HA coated samples with various number of pulsed laser

samples with comparison to samples in artificial saliva, these results agreement with fact that the corrosion resistance of pure metal or an alloy strongly depends on the environment where it is exposed, the chemical composition, viscosity and so forth (Ghaith *et al*., 2015). It's clear also, that the samples showed relatively similar behavior to that observed in saliva solution such as the corrosion resistance of 316 L st.st sample with HA coating is higher than that for 316 L st.st uncoated sample. This result agree with Nawal (2014).

Ni release results: Though Ni is an essential element for the human body, it is allergenic and toxic when present at elevated levels. Nickel ion release was measured for coated and uncoated samples by using atomic absorption spectrometry in artificial saliva and hanks solution at 3°C for 15 days. Nickel ion release concentration in artificial saliva show in Fig. 15 of the (A) sample was (0.5671 ppm), the lowest corresponding number of coated sample is (0.1194). This means that an improvement of (78.94%) is introduced by HA coated. However, it appears that a further improvement was obtained by the increase of number of pulses higher number of pulses lower of Nickel ion release number. Therefore, the increase of pulses from (3000-6000) causes a decrease of (0.1332-0.1194), i.e., an improvement of (10.36%) was obtained Fig. 15. This enhancement in reducing nickel release is more likely due to HA layer provide an adherent and very protective layer which suppresses the Ni ion releasing because it isolates the surface completely from its surrounding. Table 10 the

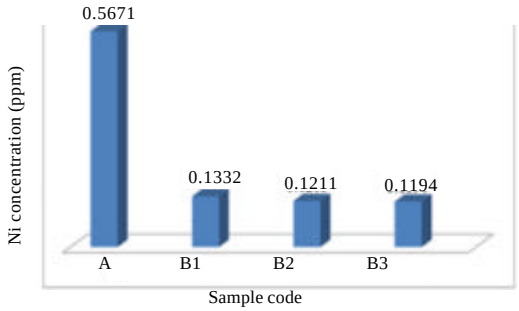

Fig. 15: Nickel ion concentration values for the coated sample and the uncoated samples with various number of pulses in artificial saliva and at 37°C for 15 days

Table 10: The amount of Ni concentration in artificial saliva at 37°C

Samples code	Ni concentration (ppm)
A	0.5671
B1	0.1332
B2	0.1211
B3	0.1194

amount of Ni concentration after immersion in artificial saliva for 15 days Nickel ion release concentration in hanks solution show in Fig. 16 of the uncoated sample was (10.4179 ppm), the lowest corresponding number of coated sample was (0.2686). This means that an improvement of (97.42%) is introduced by HA coated. The HA coating can effectively suppress leaching of metal ions to the biological solutions. Table 11 the amount of Ni concentration after immersion in Hank's solution for 15 days.

Table 11: The amount of Ni concentration in Hank's solution

Samples code	Ni concentration (ppm)
A	10.4179
B1	0.4234
B2	0.3265
B3	0.2686

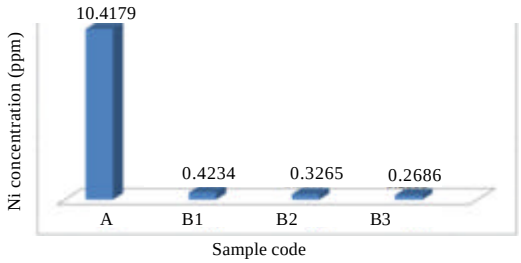

Fig. 16: Nickel ion concentration values for the coated and uncoated samples with various number of pulses in Hank's solution and at 37°C for 15 days

CONCLUSION

Based on the obtained result, the following conclusion are made: corrosion resistance of HA coated samples was greatly improved. For instance an improvement of (97.6%) in synthetic saliva. In Hanks solution, however, the improvement in corrosion resistance was (96.30%). A great reduction in Ni-release was observed in the research an enhancement of reduction of (78.94%) in synthetic saliva occurs. In hanks solution the Ni-release enhancement was (97.42%).

REFERENCES

Ajay, S. and R. Abhinandan, 2010. Study of hydroxyapatite and hydroxyapatite-chitosan composite coatings on stainless steel by electrophoretic deposition method. Master Thesis, National Institute of Technology, Rourkela, India.

Balla, V.K., M. Das, S. Bose, G.J. Ram and I. Manna, 2013. Laser surface modification of 316 L stainless steel with bioactive hydroxyapatite. Mater. Sci. Eng. C., 33: 4594-4598.

Ghaith, E.S., S. Hodgson and M. Sharp, 2015. Laser surface alloying of 316L stainless steel coated with a bioactive hydroxyapatite-titanium oxide composite. J. Mater. Sci. Med., Vol. 26, 10.1007/s10856-015-5399-1

Hermawan, H., D. Ramdan and J.R.P. Djuansjah, 2011. Metals for biomedical applications. Master Thesis, Faculty of Biomedical Engineering and Health Science, University Teknologi Malaysia, Johor Bahru, Malaysia.

Kwok, C.T., P.K. Wong, F.T. Cheng and H.C. Man, 2009. Characterization and corrosion behavior of hydroxyapatite coatings on Ti6Al4V fabricated by electrophoretic deposition. Appl. Sur. Sci., 255: 6736-6744.

Nawal, M.D., 2014. Preparation and characterization of bio nitinol with addition of Copper. Ph.D Thesis, Materials Engineering Department, University of Technology, Iraq, Baghdad, Iraq.

Ng, K.W., H.C. Man and T.M. Yue, 2011. Characterization and corrosion study of NiTi laser surface alloyed with Nb or CO. Appl. Surf. Sci., 257: 3269-3274.

Ohtsuki, C., 2011. How to prepare the Simulated Body Fluid (SBF) and its related solutions, proposed by Kokubo and his colleagues. BA. Thesis, Kyoto University, Kyoto, Japan.

Okazaki, Y., E. Gotoh, T. Manabe and K. Kobayashi, 2004. Comparison of metal concentrations in rat tibia tissues with various metallic implants. Biomater., 25: 5913-5920.

Puleo, D.A. and W.W. Huh, 1995. Acute toxicity of metal ions in cultures of osteogenic cells derived from bone marrow stromal cells. J. Appl. Biomater., 6: 109-116.

Shalabi, M.M., J.G. Wolke, V.M. Cuijpers and J.A. Jansen, 2007. Evaluation of bone response to titanium-coated polymethyl methacrylate resin (PMMA) implants by X-ray tomography. J. Mater. Sci. Mater. Med., 18: 2033-2039.

Singh, R. and N.B. Dahotre, 2007. Corrosion degradation and prevention by surface modification of biometallic materials. J. Mater. Sci. Med., 18: 725-751.

Smausz, T., B. Hopp, H. Huszar, Z. Toth and G. Kecskemeti, 2004. Pulsed laser deposition of bioceramic thin films from human tooth. Appl. Phys. A., 79: 1101-1103.